ACS Catalysis

Research Article

pubs.acs.org/acscatalysis

One-Pot Synthesis of Pd Nanoparticle Catalysts Supported on N-Doped Carbon and Application in the Domino Carbonylation

Zelong Li,[†,‡] Jianhua Liu,[†] Zhiwei Huang,[†] Ying Yang,[†] Chungu Xia,*[,†] and Fuwei Li*[,†]

[†]State Key Laboratory for Oxo Synthesis and Selective Oxidation, Lanzhou Institute of Chemical Physics, Chinese Academy of Sciences, Lanzhou, Gansu 730000, P.R. China

[‡]University of the Chinese Academy of Sciences, Beijing 100049, P.R. China

Supporting Information

ABSTRACT: In this work, we report a novel and facile procedure for a one-pot preparation of palladium nanoparticle catalysts supported on porous N-doped carbon ($Pd@CN^{T}$) by direct carbonization of palladium-*N*-heterocyclic carbene coordination polymer (P-Pd-NHC). This method could be conveniently extended to the synthesis of the Ni and alloy (Pd_xNi_y) nanoparticle catalysts ($Ni@CN^{800}$, $Pd_xNi_y@CN^{800}$). The treatment temperature played an important role on the growth and properties of the resultant $M@CN^{T}$, wherein $M@CN^{800}$ carbonized at 800 °C showed well-monodispersed metal nanoparticles (MNPs), graphene-like layers of the N-doped carbon supports, and strong interaction between MNPs and the support. $Pd@CN^{800}$ displayed high efficiency and stable recyclability toward the domino carbonylative synthesis of pyrazole derivatives. Interestingly, its catalytic performance has been even higher than that of the representative $PdCl_2(PPh_3)_2$ within six runs.

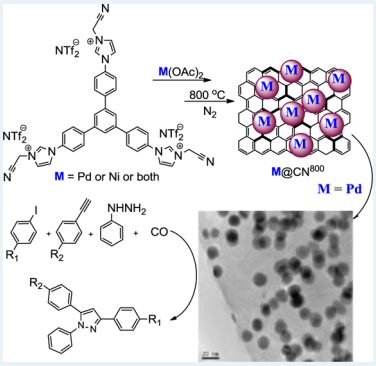

KEYWORDS: *N-doped carbon, N-heterocyclic carbenes, supported catalysts, nanoparticles, carbonylation*

1. INTRODUCTION

Recently, the synthesis of supported MNPs as heterogeneous catalyst for liquid phase reactions has attracted extensive research interests.[1−3] Impregnation and coprecipitation are commonly used methods to prepare these supported catalysts, however, either the aggregation of MNPs or the irreversible leaching of metal atoms from the supports during the reaction will inevitably reduce their catalytic activity and stability, which are also the limitations of the postloading methodology to the practical applications. Additionally, the preparation of such a kind of catalysts usually needs to use excess reducing reagents such as $NaBH_4$ and $LiAlH_4$ resulting inorganic wastes. Therefore, the development of methodology to expediently synthesize active and stable supported MNPs for liquid phase reactions is highly desirable.[1,4]

Nanostructured porous carbon materials have been the popular catalytic supports due to their high surface area and good stability.[5−15] It is known that traditional carbons (including carbon black, activated carbon, carbon nanofibers, and carbon nanotubes) are poor in functional groups, and so their supported MNPs by ordinary impregnation often result in aggregation or leaching of the particles in the liquid solution because of the weak interaction between MNPs and the carbon supports. A possible solution to enhance the catalytic performance and the stability of such kinds of catalysts is the introduction of functional groups (e.g., nitrogen groups) on the surface of the supports.[16−19] Among the procedures used to synthesize nitrogen-doped (N-doped) carbons, in situ doping by using nitrogen-containing precursors can realize a homogeneous incorporation of nitrogen into carbons. Following such a direct carbonization method, Antonietti, Dai and their co-authors have prepared functional N-doped carbons.[20−24] These N-doped carbon materials themselves have shown novel physicochemical properties and could be better supports to stabilize and disperse MNPs for the postpreparation.[10,12,25,26] However, to the best of our knowledge, no one-pot synthesis of MNP catalysts supported on N-doped carbon without using any reducing agents has ever been reported.

Transformations of rationally synthesized molecular compounds to materials constitute an important new direction in both structural inorganic chemistry and materials chemistry, which will enable possible pathways for the rational design of materials.[27] Based on this concept, in situ carbonization of structurally defined organometallic coordination polymers containing both nitrogen and metal atoms could possibly be an option for one-step preparation of metal-supported N-doped carbon catalytic materials. Additionally, high carbonization yields, a certain amount of functional groups loading, and homogeneous distributions of MNPs in the carbon matrix are also the important key factors for the development of a procedure to synthesize such catalytic material.[23] In the past decade, N-heterocyclic carbene (NHC) metal complexes have found a wide range of applications in catalysis and material.[28,29] We herein report a facile one-pot synthesis of (hetero)metallic-

Received: January 30, 2013
Revised: March 18, 2013
Published: March 19, 2013

(Ni, Pd, or Ni_xPd_y) nanoparticles supported N-doped carbon catalytic materials from the corresponding (hetero)metal−NHC coordination polymers. Such a kind of supported catalysts displayed narrow metal size distribution, good stability, and efficient catalytic activity toward a four-component cascade carbonylation reaction to yield heterocyclic pyrazole.

On the basis of our and other reported knowledge,[30−33] transition metal acetate salts, such as $Pd(OAc)_2$ and $Ni(OAc)_2$, could easily react with imidazolium C2−H of the NHC precursor to form a M−C bond, which could be a bridge to intermolecularly link polydentate NHCs and generate a coordination polymer. Meanwhile, Dai and co-workers have found that the nitrile arm of an ionic liquid is a key to attain high carbon yields of the resultant metal-free carbon nitride materials.[34,35] It is assumed that a metal−NHC coordination polymer with functional nitrile arms could be an ideal precursor for the one-pot preparation of metal-supported N-doped carbon catalysts via high temperature carbonization, by which the carbon, nitrogen atoms, and MNPs would be homogeneously reassembled to form MNP embedded N-doped carbon catalysts.

2. EXPERIMENTAL SECTION

2.1. Synthesis of P-M-NHC. A novel and tridentate NHC precursor, $[TPBAIm][NTf_2]_3$, with functional nitrile arms was initially prepared in high yield from readily accessible starting materials [Scheme S1 in the Supporting Information]. Subsequently, as shown in Scheme 1, $[TPBAIm][NTf_2]_3$ and

Scheme 1. Synthesis of P-M-NHC and M@CN^T

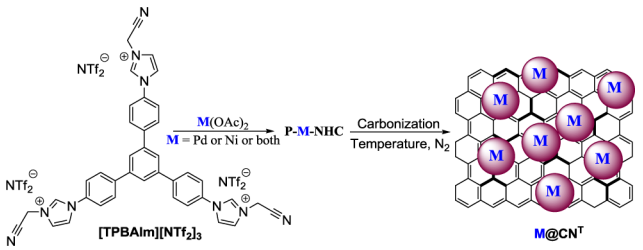

1.5 equiv of $Pd(OAc)_2$ or $Ni(OAc)_2$ or their mixture with a certain mole ratio were dissolved in 10 mL of DMF with the presence of 3.6 equiv of NaOAc and were stirred at 110 °C for 24 h. A pale yellow precipitate was formed, and the precipitate was isolated by filtration and rinsed with DMF (3 × 30 mL) and EtOH (3 × 30 mL) to remove unreacted salts. Solvent was removed by heating the material at 150 °C for 24 h under vacuum to yield the desired P-M-NHC. Taking P-Pd-NHC as an example, $[TPBAIm][NTf_2]_3$ (1.0 mmol) reacted with $Pd(OAc)_2$ (1.5 mmol) in the presence of NaOAc (3.6 mmol) in 10 mL of DMF at 110 °C. Finally, 970 mg of P-Pd-NHC was isolated.

2.2. Synthesis of M@CN^T. The carbonization was performed under N_2 atmosphere. A certain amount of specific P-M-NHC was introduced into a quartz tube, and the temperature was controllably ramped at a rate of 10 °C min^{-1} to a final temperature (300, 400, and 800 °C), and then the final temperature was maintained for 1 h to finish the one-pot synthesis of monometallic or bimetallic nanoparticle catalysts supported N-doped porous carbon, generally named as M@CN^T, wherein CN represents N-doped carbon support, M stands for Ni or Pd or Pd_xNi_y, and T is the carbonization temperature. Additionally, for the sake of comparison, the ligand precursor $[TPBAIm][NTf_2]_3$ was also similarly carbonized at 800 °C under N_2 for 1 h, and the product was named as LP^{800}.

2.3. Material Characterization. NMR spectra were obtained on a BRUKER DRX spectrometer operating at 400 MHz for ^1H NMR and 100 MHz for ^{13}C NMR. Chemical shifts are reported in parts per million (ppm) downfield from TMS with the solvent resonance as the internal standard. Coupling constants (J) are reported in Hz and refer to apparent peak multiplications. High resolution mass spectra (HRMS) were recorded by Bruker microTOF-II (ESI). Elemental analyses were carried out on a Vario EL analyzer. Inductively coupled plasma atomic emission spectrometry (ICP-AES) was performed on a Shimadzu ICPS-8100 equipment by the chemical analysis team in RIKEN. The detection of palladium content was carried out on an Atomic absorption spectroscopy (AAS), and its model is 180-80. Powder X-ray diffraction (XRD) measurements were performed using an X'Pert Pro multipurpose diffractometer (PANalytical, Inc.) with Ni-filtered Cu Kα radiation (0.15046 nm) at room temperature from 10.0° to 80.0° (wide angle). Measurements were conducted using a voltage of 40 kV, current setting of 40 mA, step size of 0.02°, and count time of 4 s. The nitrogen adsorption and desorption isotherms at −196 °C were recorded on an Autosorb-iQ analyzer (Quantachrome Instruments, Boynton Beach, FL). Prior to the tests, samples were degassed at 200 °C for 4 h. The specific surface areas were calculated via the BET method in the relative pressure range of 0.05−0.3, and the single-point pore volume was calculated from the adsorption isotherm at a relative pressure of 0.990. Transmission electron microscopy and high resolution transmission electron microscope (TEM, HRTEM) experiments were conducted in a JEM-2010 TEM with an accelerating voltage of 300 kV. X-ray photoelectron spectroscopy (XPS) analyses of the catalysts were performed on a Thermo Fisher Scientific K-Alpha spectrometer. Thermogravimetric−differential scanning calorimetry (TG−DSC) measurements were carried out on a NETZSCH STA 449F3 thermogravimetric analyzer from room temperature to 800 °C at a rate of 10 °C/min under nitrogen atmosphere.

2.4. Catalytic Application in the Domino Carbonylation. Representative Pd@CN^{800} (0.01 mmol), iodobenzene (0.5 mmol), phenylacetylene (0.60 mmol), phenyhydrazine (0.65 mmol), Et_3N (1.0 mmol), and 1.5 mL of MeOH were introduced into a 50 mL Schlenk tube with a magnetic bar, and then the glass tube was vacuumed and purged with CO (99.99% purity) three times before it was finally pressurized with 1.0 atm of CO gas. Subsequently, the reaction mixture was stirred at 70 °C for 6 h. After cooling to room temperature, excess CO was carefully released and the crude product was purified by flash chromatography on silica gel with petroleum ether/ethyl acetate (10:1) as eluent to afford the pyrazole product.

After the completion of the fresh reaction performed with the above typical procedure, the liquid reaction mixture was separated from Pd@CN^{800} catalyst through centrifugation, and the residual solid catalyst could be reused for the next run after addition of fresh reactants.

3. RESULTS AND DISCUSSION

The MNP catalysts supported on N-doped carbon, M@CN^{800} (M = Pd, Ni), carbonized at 800 °C were initially prepared, and their structure and morphology were characterized by transmission electron microscopy (TEM), as shown in Figure 1a,e

dx.doi.org/10.1021/cs400077r | ACS Catal. 2013, 3, 839−845

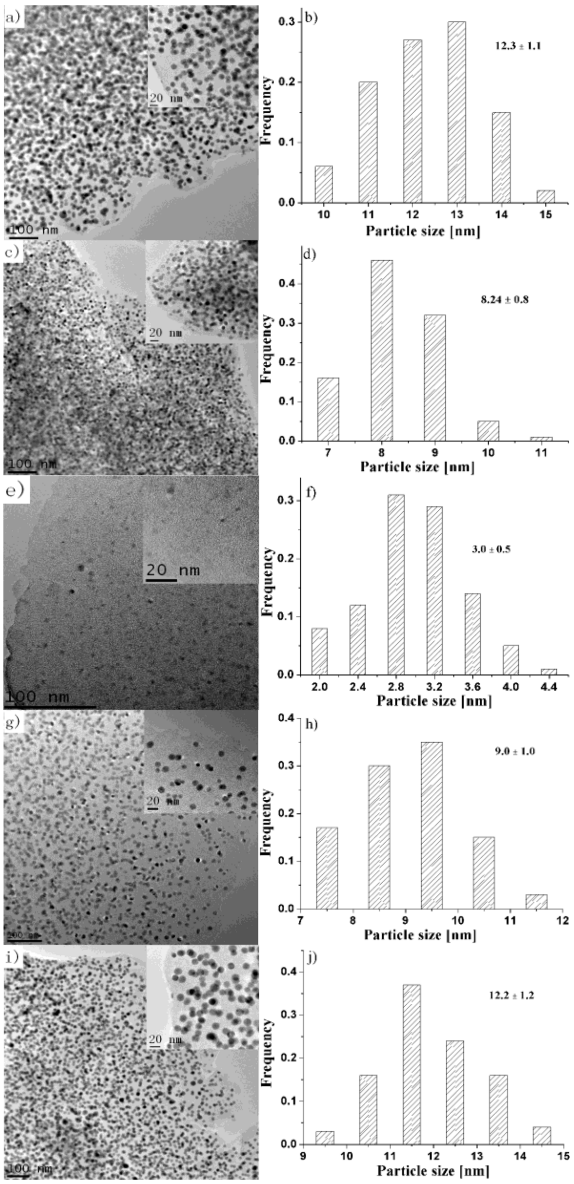

Figure 1. TEM pictures and metal nanoparticle size distribution of (a and b) Pd@CN^{800}. (c and d) Pd@CN^{400}. (e and f) Ni@CN^{800}. (g and h) $Pd_{80}Ni_{20}$@CN^{800}. (i and j) recycled catalyst (Pd@CN^{800}) after six runs.

and Supporting Information Figures S1 and S2, the PdNPs in Pd@CN^{800} and NiNPs in Ni@CN^{800} are well monodispersed in different graphene-like layers of the N-doped carbon supports and possess a uniform size ditribution, which are quite narrow with 12.3 ± 1.1 nm for PdNPs (300 nanoparticles, Figure 1b) and 3.0 ± 0.5 nm for NiNPs (Figure 1f), respectively. Interestingly, this facile method could apply not only to the synthesis of monometallic MNP-supported N-doped carbons but also to the preparation of bimetallic nanostructured catalytic materials by carbonization corresponding P−Pd_xNi_y-NHC with a certain metal ratio. It is revealed in Figure 1g,h and Supporting Information Figure S3 that the $Pd_{80}Ni_{20}$NPs of $Pd_{80}Ni_{20}$@CN^{800} are also homogeneously dispersed in the N-doped carbon matrix and their diameter is finely controlled at around 9.0 ± 1.0 nm, which is between the diameter of monometallic NiNPs and PdNPs. Susequently, representative Pd_xNi_y@CN^{800} with different Pd and Ni ratios could be easily prepared in high yields. TEM analysis of $Pd_{50}Ni_{50}$@CN^{800} and $Pd_{20}Ni_{80}$@CN^{800} in Supporting Information Figures S4 and S5 showed that the alloy nanoparticles could also be well-monodispersed in the resultant N-doped carbon supports. Additionally, as presented in Figure 2, the X-

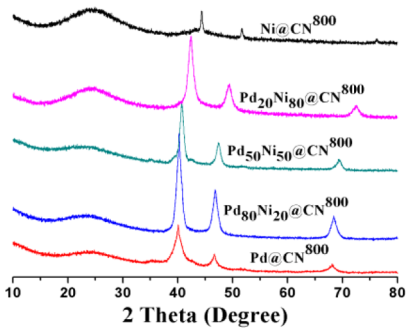

Figure 2. Wide-angle XRD patterns of Pd_xNi_y@CN^{800}.

ray diffraction (XRD) patterns of Ni@CN^{800}, Pd@CN^{800}, and Pd_xNi_y@CN^{800} further proved that the monometallic PdNPs, NiNPs, and bimetallic Pd_xNi_y alloy nanoparticles have been successfully obtained. All these characterizations indicate that the direct carbonization of structure-defined and readily synthesized metal−NHC coordination polymers is a facile and general methodology to prepare monometallic- and heterometallic-MNPs supported N-doping carbon materials.

To gain more information about the formation of the nanoparticles, monometallic Pd@CNT was taken as model samples to investigate further. Though the PdNPs loading for Pd@CN800 was as high as 24% estimated by atomic absorption spectroscopy (AAS), it was observed that the PdNPs were homogeneously embedded on the nanostructured N-doped carbon supports from the TEM results. Furthermore, the well-dispersed small metal nanoparticles could also be clearly seen from the STEM-HAADF image (Supporting Information Figure S1c) of Pd@CN800. It could be calculated from the high-resolution TEM (HRTEM, Supporting Information Figure S1d) image of the Pd@CN800 that the interplanar spacing of the PdNPs particle lattices is 0.23 nm, which matched well with the (111) lattice spacing of face-centered cubic (fcc) Pd. A good indication of the growth mechanism of such a kind of MNP-supported carbon catalysts came from the differences of PdNPs size distribution and N-doped carbon matrix morphology of Pd@CN^{400} and Pd@CN^{800}, and smaller and narrower PdNPs size distribution with 8.2 ± 0.8 nm could be obtained in Pd@CN^{400} (Figure 1d); however, its supports displayed an amorphous morphology while the supporting matrix of Pd@CN^{800} exhibited layered graphene-like structure (Figure 1c), which suggested that the carbonization temperature played a crucial role in the syntheses of these catalytic materials. Additionally, it could be speculated that the formation of PdNPs was initiated by the cleavage of the Pd−C bond and then Pd, C, and N atoms were assembling to grow to the optimal structured PdNPs supported N-functional carbon with the increasing temperature.

The carbonization yield is also an important factor for the material synthetic method; as shown in Table 1, the yield of LP^{800} through carbonization of [TPBAIm][NTf_2]$_3$ at 800 °C is 37 wt %, and the formation of organometallic coordination polymer (P-Pd-NHC) could effectively enhance the carbonization yield to 58 wt %, affording structually optimized Pd@

dx.doi.org/10.1021/cs400077r | ACS Catal. 2013, 3, 839−845

Table 1. Characteristics of LP^{800} and $Pd@CN^{T}$

sample	carbonization yield (%)	S_{BET} ($m^2\ g^{-1}$)	V_{BJH} ($cm^3\ g^{-1}$)
LP^{800}	37	667	0.50
$Pd@CN^{400}$	90	344	0.17
$Pd@CN^{800}$	58	395	0.19

CN^{800}. Due to the similar manipulation procedure, thermogravimetric analysis (TGA) could be a good tool to detect the carbonization process of $[TPBAIm][NTf_2]_3$ and P-Pd-NHC. It is revealed in Figure 3A that their decomposition occurred in

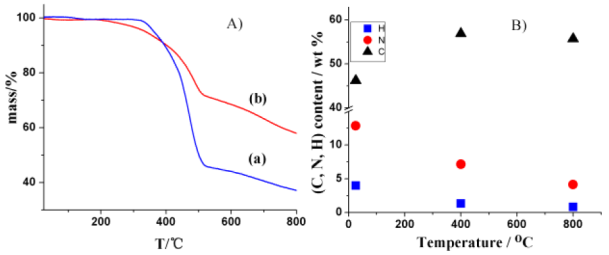

Figure 3. (A) TG curves of (a) $[TPBAIm][NTf_2]_3$; (b) P-Pd-NHC under N_2 with a heating rate of 2 °C min^{-1}. (B) C, N, and H content of P-Pd-NHC, $Pd@CN^{400}$, $Pd@CN^{800}$ determined by elemental analysis (EA).

two distinct steps, the first stage of $[TPBAIm][NTf_2]_3$ started at 337 °C, and P-Pd-NHC proceeded to decompose at a lower temperature (225 °C) possibly due to the initial disconnection of coordinative Pd-OAc bonds in the P-Pd-NHC; both of their first decomposition stages weren't completed until 500 °C. Their second decomposition phases were similar, ranging from 500 to 800 °C. The C, N, and H content variations of P-Pd-NHC, $Pd@CN^{400}$, and $Pd@CN^{800}$ detected by EA are shown in Figure 3B; when the temperature increased from 400 to 800 °C, the N content decreased from 7.15 to 4.45 wt % and H content decreased to 0.85 wt %. These variations possibly indicated that the carbon nitride matrix reconstructed to form the proper ring system to fit the requirements of the locally graphitized structure, which is also in accordance with the TEM results showing the carbon nitride matrix changing from amorphous morphology for $Pd@CN^{400}$ to the layered graphene-like structure of $Pd@CN^{800}$. N_2 adsorption−desorption isotherms for LP^{800}, $Pd@CN^{400}$, and $Pd@CN^{800}$ are given in Figure 4. Compared with $Pd@CN^{400}$, the nitrogen sorption

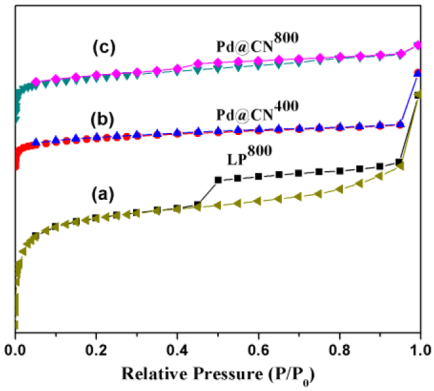

Figure 4. Nitrogen sorption of (a) LP^{800}, (b) $Pd@CN^{400}$, and (c) $Pd@CN^{800}$.

isotherms of $Pd@CN^{800}$ and LP^{800} exhibit a type-H2 hysteresis loop, indicating the presence of mesoporosity. However, when the Pd nanoparticles are introduced into $Pd@CN^{800}$, its specific surface area and the pore volume fell dramatically (Table 1).

Figure 5a showed the XRD patterns of P-Pd-NHC and its carbonized $Pd@CN^{T}$ at different temperatures. P-Pd-NHC

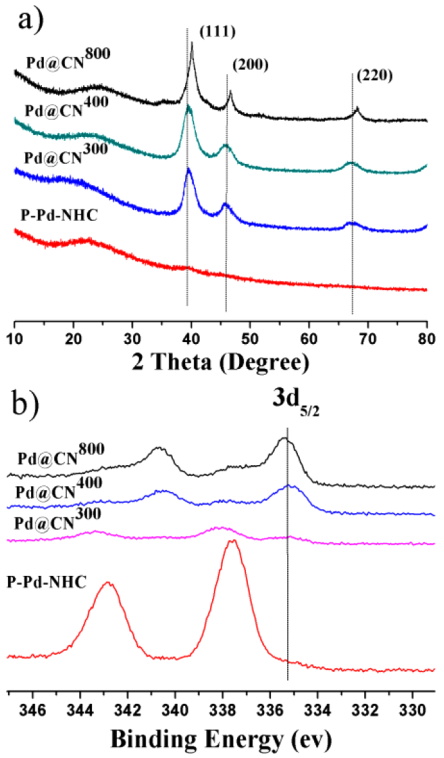

Figure 5. (a) Wide-angle XRD pattern of $Pd@CN^{T}$; (b) Pd 3d XPS spectra of $Pd@CN^{T}$.

precursor only displayed a broad band at ca. 25°, indicating its amorphous nature and Pd^{2+} oxidation state of the coordination polymer. After P-Pd-NHC was carbonized to $Pd@CN^{T}$, three well-resolved peaks were obversed in $Pd@CN^{300}$, $Pd@CN^{400}$, and $Pd@CN^{800}$, respectively. The sharper peaks of the XRD patterns for $Pd@CN^{800}$ proved that the highly crystalline face-centerd cubic (fcc) Pd nanoparticles were obtained. The slightly broad peaks for $Pd@CN^{300}$ and $Pd@CN^{400}$ shifted to lower values, which indicated that the PdC_x phase was formed during carbonization at 300 and 400 °C. These phenomena were consistent with the previous reports that the littice parameter of bulk Pd with carbon occupying interstitial octahedral sites has increased.[36−38] And when enhancing the treatment temperature to 800 °C under inert atmosphere, the interstitial carbon atoms would be expelled from the palladium lattice to form pure PdNPs.[36−38]

X-ray photoelectron spectroscopy (XPS) analysis was also used to study the variation of the Pd oxidation state in the precursor and resultant $Pd@CN^{T}$ catalysts. As shown in Figure 5b, the Pd 3d photoelectron spectrum of P-Pd-NHC showed two peaks around 342.8 and 337.6 eV in the $3d_{3/2}$ and $3d_{5/2}$ levels, indicating the Pd species in the polymer precursor are Pd^{2+} state, which was also proved by previous XRD analysis. Although the XPS patterns of $Pd@CN^{300}$ were still dominated by Pd^{2+} oxidation state, characteristic Pd^{0} species with $3d_{5/2}$ spin−orbit components at 335.0 and 335.5 eV assignable to

dx.doi.org/10.1021/cs400077r | ACS Catal. 2013, 3, 839−845

metallic Pd and carbon-diffused PdC_x surface phase, respectively, started to be generated after heat treatment for P-Pd-NHC at 300 °C (Supporting Information Figure S6a). XPS measurment of $Pd@CN^{400}$ showed most of the Pd species presented as Pd^0 nanoparticles with a small amount of oxidized Pd atoms in the N-doped carbon matrix (Supporting Information Figure S6b). Upon enhancing the carbonization temperature to 800 °C, the characteristic Pd photoelectron peaks indicated that the majority (roughly 81% based on XPS) of the Pd species are well-crystallized Pd^0 nanoparticles (Supporting Information Figure S6c). It was reported that the introduction of amine groups possessing electron-donor properties in the carbon carrier can stabilize high-dispersed Pd^0 and prevented its reoxidation.[39] In our case, the status of N in $Pd@CN^{300}$, $Pd@CN^{400}$, and $Pd@CN^{800}$ can also be explored by XPS analysis of N 1s; as shown in Figure 6a and Supporting

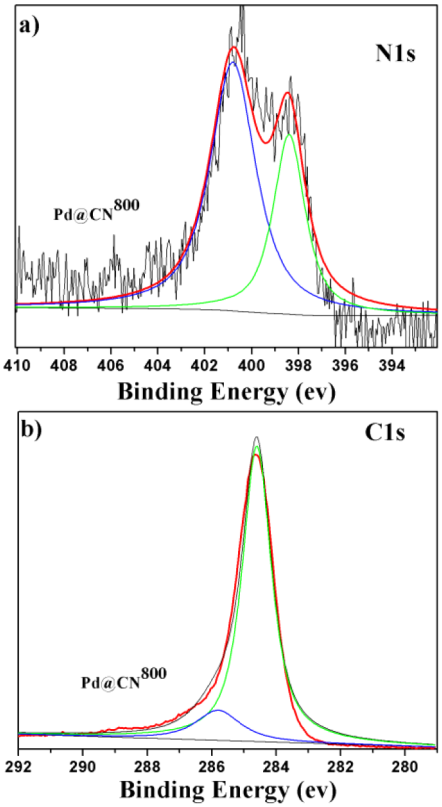

Figure 6. XPS analysis of $Pd@CN^{800}$: (a) N 1s and (b) C 1s.

Information Figure S7, the N 1s spectra could be divided into two peaks, one peak at 398.4 eV ascribed to pyridine-like sp^2 nitrogen and another 400.9 eV peak attributed to the quaternary nitrogen.[40,41] Therefore, the pyridinic nitrogen atoms along with the quaternary nitrogen in planar C−N−C-layers in our system can stabilize high-dispersed Pd^0 to prevent efficiently the reoxidation of the Pd atoms.[26,39] When a nitrogen atom is doped into carbon materials, the charge distribution of the carbon atoms will be influenced by the neighbor nitrogen dopants.[42] Hence, the C 1s spectrum for $Pd@CN^{800}$ could also be deconvoluted into two peaks centered at 284.6 and 285.8 eV, corresponding to pure graphitic sites in the CN matrix and sp^2 carbon atoms bonded to the nitrogen inside the aromatic structure, respectively (Figure 6b).[43,44]

In the present series of $Pd@CN^T$ catalysts, strong metal−support interaction between Pd nanoparticle and the carbon nitride support can be speculated from the characteristic XPS peak at 335.5 eV, which could be attributed to the PdCx phase formation[45,46] and the interactions[47] between Pd nanoparticles and the carbon nitride matrix in $Pd@CN^{300}$ and $Pd@CN^{400}$; the Pd $3d_{5/2}$ XPS peak at 335.5 eV of $Pd@CN^{800}$ was exclusively induced by the strong interaction between Pd nanoparticles and N-doped carbon support since the PdCx phase that formed in lower temperature has been transferred into metallic Pd nanoparticles. Therefore, treatment of the organometallic coordination polymers homogeneously containing nitrogen and metal atoms could possibly be an alternative to realize the high dispersion of the nitrogen and MNPs in the carbon materials through their chemically assembling growth and thus increase the interaction between MNPs and supports. It is important to note that, comparing with PdC_x species, the pure Pd nanoparticles possibly show higher reactivity toward the oxidative addtion of Pd^0 onto the C−X bond during the catalytic transformation of aryl halide.

Multicomponent domino reactions are among the most powerful synthetic tools available because they allow rapid access to structural variation and complexity in a single reaction vessel without intermediary purification steps.[48−50] However, those transformations are mainly achieved by the homogeneous catalysis of a noble metal catalyst and thus a recyclable catalyst system will promote it to be a more competitive and economical tool, especially in the preparation of heterocyclic compounds. Pyrazole, a five-membered heterocycle with two adjacent nitrogen atoms, has attracted considerable interests in medicinal and coordination chemistry.[51−54] Mori and co-authors[55] developed a homogeneous Pd-catalyzed four-component coupling carbonylation of aryl iodide, terminal alkyne, and hydrazine to yield substituted pyrazole (see Table 2), but such a method failed in the reaction with arylhydrazine. Later, Stonehouse et al.[56] disclosed another similar catalytic procedure replacing CO gas with solid $Mo(CO)_6$ as carbonyl resource, however, with phenylhydrazine only giving 47% yield of the corresponding triaryl substituted pyrazole. One of the

Table 2. One-Pot Four-Component Synthesis of Pyrazoles[a]

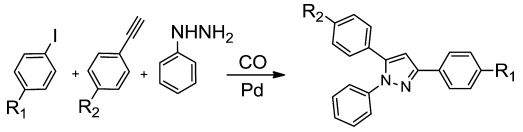

entry	catalyst	R_1	R_2	yield[b] (%)
1	$Pd@CN^{800}$	H	H	92
2	$Pd@CN^{300}$	H	H	36
3	$Pd@CN^{400}$	H	H	62
4	$PdCl_2(PPh_3)_2$	H	H	83
5	$Pd@CN^{800}$	H	F	88
6	$Pd@CN^{800}$	H	*t*-Bu	81
7	$Pd@CN^{800}$	Cl	H	83
8	$Pd@CN^{800}$	Cl	F	93
9	$Pd@CN^{800}$	Cl	*t*-Bu	86
10	$Pd@CN^{800}$	Me	H	92
11	$Pd@CN^{800}$	Me	F	93
12	$Pd@CN^{800}$	Me	*t*-Bu	88
13[c]	$Pd@CN^{800}$	H	H	84

[a]Reaction conditions: iodobenzene (0.5 mmol), arylacetylene (0.60 mmol), phenyhydrazine (0.65 mmol), catalyst (2.0 mol %), Et_3N (1.0 mmol), MeOH (1.5 mL), CO (1.0 atm), temperature (110 °C), and reaction duration (6 h). [b]Isolated yield. [c]Hydrazine hydrate.

dx.doi.org/10.1021/cs400077r | ACS Catal. 2013, 3, 839−845

key factors of this tandem catalytic syntheis is to develop an active Pd^0 catalyst to initiate its oxidative addition onto the aryl C−X bond, and this catalyst requirement matches well with the property of present Pd@CN^{800}, which has very high and widely dispered Pd^0 metallic nanoparticle proportion as well as the stability support through the interaction with the N-doped porous carbon materials. To verify this assumption and furthur our ongoing interest on the Pd-catalyzed carbonylation reactions,[57−61] four-component carbonylation of iodobenzene, phenylacetylene, phenylhydrazine, and CO gas was selected as a model reaction to test the catalytic performance of the heterogeneous Pd@CN^T catalysts. Such a cascade reaction would be an initial carbonylative Sonogashira coupling between benzene iodide and aryl alkyne to yield α,β-alkynyl ketone,[55,62] followed by the addition and cyclic condensation with phenylhydrazine to give the desired pyrazole product.[63−66]

To our delight, as shown in Table 2, Pd@CN^{800} demonstrated efficient activity toward the one-pot synthesis of triaryl substituted pyrazole, giving a 92% yield under 1.0 atm pressure of CO gas (Entry 1). However, its analogues carbonized at lower temperature, Pd@CN^{300} and Pd@CN^{400}, only showed low to moderate activities (Entries 2 and 3). These catalytic activity differences are consistent with their properties of the corresponding Pd@CN^T based on TEM, XRD, and XPS analysis, which revealed that Pd@CN^{800} has higher proportion of well dispersed metallic Pd nanoparticles and stronger support stabilization effect. Surprisingly, the current heterogeneous catalytic system even presented higher reactivity than that of the representative homogeneous carbonylation catalyst, $PdCl_2(PPh_3)_2$, which yielded 85% of the triphenyl-substituted pyrazole (Entry 4). This is possible because the current cascade reaction is initiated by a Pd^0 species, and the homogeneous Pd^{2+} complex needs to be reduced to Pd^0 before it can undergo the oxidative addition onto the C−X bond of aryl halide. Furthermore, the present Pd nanoparticles catalyst supported N-doped carbon displayed good substrate tolerance, and iodobenzenes and phenylacetylenes with different electronic donating or withdrawing substituents all worked perfectly with high isolated yields of the desirable pyrazoles (Entries 5−12, 81−93%). Besides phenylhydrazine, the cascade carbonylative coupling reaction with the simple hydrazine could also proceed efficiently, giving an 84% yield of the expected biaryl-substituted pyrazole (Entry 13).

Besides efficient catalytic acitivity, stable recyclability is also crucial for an outstanding heterogeneous catalyst from the viewpoint of both academic research and industrial applications. As shown in Figure 7, Pd@CN^{800} demonstrated high stability and could be used at least six times by simple centrifugation without a significant loss of its catalytic performance. To further verify its stability, Pd concentration in the reaction solution was determined by ICP-AES to be less than 0.1 ppm, indicating that leaching of Pd into the liquid phase is negligible. Moreover, TEM anlaysis of the reused catalyst revealed that the dispersion and size distribution of PdNPs did not show any obvious change after six runs (Figure 1g,f) compared with the fresh catalysts (Figure 1a,b). As expected, the nitrogen functionalities on the carbon matrix might act as a coordination donor ligand to tune the electronic property of PdNPs and thus enhance its stability as well as the catalytic activity.

4. CONCLUSION

In summary, a facile one-pot methodology to prepare metallic and heterometallic nanoparticle catalysts supported on porous

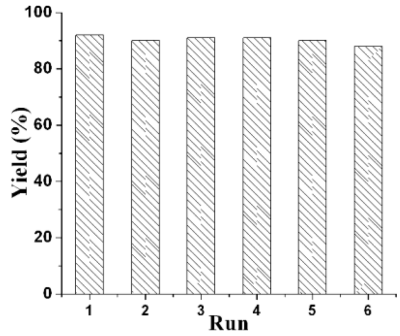

Figure 7. Recycle of the catalyst Pd@CN^{800}. Reaction conditions: iodobenzene (0.5 mmol), phenylacetylene (0.60 mmol), phenyhydrazine (0.65 mmol), Pd@CN^{800} (2.0 mol %), Et_3N (1.0 mmol), MeOH (1.5 mL), CO (0.1 MPa), temperature (110 °C), and reaction duration (6 h).

N-doped carbon by direct carbonization of a metal−NHC coordination polymer has been successfully developed. Deep investigations revealed that treatment temperature played an important role on the growth and properties of the resultant M@CN^T. The novel Pd catalyst, Pd@CN^{800}, displayed high activity and selectivity toward the domino carbonylative synthesis of pyrazole derivatives from three simple substrates and an atmosphere pressure of CO gas. Its outstanding catalytic performance has been even higher than that of the representative Pd^{2+} homogeneous catalyst within six runs. These promising characters of M@CN^T and their facile preparative method will prompt us to prepare more (hetero) metallic nanoparticle supported catalysts and investigate their sustainable catalysis in the further research.

■ ASSOCIATED CONTENT

Ⓢ Supporting Information

The details of the preparation of materials and their characterizations, catalytic procedures, and NMR spectra for the pyazole products. This material is available free of charge via the Internet at http://pubs.acs.org.

■ AUTHOR INFORMATION

Corresponding Author

*E-mail: fuweili@licp.cas.cn (F.L.), cgxia@licp.cas.cn (C.X.).

Notes

The authors declare no competing financial interest.

■ ACKNOWLEDGMENTS

This work was supported by the Chinese Academy of Sciences and the National Natural Science Foundation of China (21002106 and 21133011).

■ REFERENCES

(1) De Rogatis, L.; Cargnello, M.; Gombac, V.; Lorenzut, B.; Montini, T.; Fornasiero, P. *ChemSusChem* **2010**, *3*, 24−42.
(2) Molnár, Á. *Chem. Rev.* **2011**, *111*, 2251−2320.
(3) Guerra, J.; Herrero, M. A. *Nanoscale* **2010**, *2*, 1390−1400.
(4) Balanta, A.; Godard, C.; Claver, C. *Chem. Soc. Rev.* **2011**, *40*, 4973−4985.
(5) Zlotea, C.; Cuevas, F.; Paul-Boncour, V. r.; Leroy, E.; Dibandjo, P.; Gadiou, R.; Vix-Guterl, C.; Latroche, M. *J. Am. Chem. Soc.* **2010**, *132*, 7720−7729.
(6) Scheuermann, G. M.; Rumi, L.; Steurer, P.; Bannwarth, W.; Mülhaupt, R. *J. Am. Chem. Soc.* **2009**, *131*, 8262−8270.

(7) Chan-Thaw, C. E.; Villa, A.; Katekomol, P.; Su, D.; Thomas, A.; Prati, L. *Nano Lett.* **2010**, *10*, 537−541.
(8) Chan, C. W. A.; Xie, Y.; Cailuo, N.; Yu, K. M. K.; Cookson, J.; Bishop, P.; Tsang, S. C. *Chem. Commun.* **2011**, *47*, 7971−7973.
(9) Wang, W.; Wang, H.-y.; Wei, W.; Xiao, Z.-G.; Wan, Y. *Chem.—Eur. J.* **2011**, *17*, 13461−13472.
(10) Datta, K. K. R.; Reddy, B. V. S.; Ariga, K.; Vinu, A. *Angew. Chem., Int. Ed.* **2010**, *49*, 5961−5965.
(11) Sun, Z.; Sun, B.; Qiao, M.; Wei, J.; Yue, Q.; Wang, C.; Deng, Y.; Kaliaguine, S.; Zhao, D. *J. Am. Chem. Soc.* **2012**, *134*, 17653−17660.
(12) Xu, X.; Li, Y.; Gong, Y.; Zhang, P.; Li, H.; Wang, Y. *J. Am. Chem. Soc.* **2012**, *134*, 16987−16990.
(13) Yang, Y.; Chiang, K.; Burke, N. *Catal. Today* **2011**, *178*, 197−205.
(14) Ma, T.-Y.; Liu, L.; Yuan, Z.-Y. *Chem. Soc. Rev.* **2013**, DOI: 10.1039/C2CS35301F.
(15) Shen, W.; Fan, W. *J. Mater. Chem. A* **2013**, *1*, 999−1013.
(16) Goettmann, F.; Fischer, A.; Antonietti, M.; Thomas, A. *Angew. Chem., Int. Ed.* **2006**, *45*, 4467−4471.
(17) Groenewolt, M.; Antonietti, M. *Adv. Mater.* **2005**, *17*, 1789−1792.
(18) Jiang, L.; Gao, L. *Carbon* **2003**, *41*, 2923−2929.
(19) Stein, A.; Wang, Z.; Fierke, M. A. *Adv. Mater.* **2009**, *21*, 265−293.
(20) Hu, B.; Wang, K.; Wu, L.; Yu, S.-H.; Antonietti, M.; Titirici, M.-M. *Adv. Mater.* **2010**, *22*, 813−828.
(21) Paraknowitsch, J. P.; Zhang, J.; Su, D.; Thomas, A.; Antonietti, M. *Adv. Mater.* **2010**, *22*, 87−92.
(22) Zhai, Y.; Dou, Y.; Zhao, D.; Fulvio, P. F.; Mayes, R. T.; Dai, S. *Adv. Mater.* **2011**, *23*, 4828−4850.
(23) Lee, J. S.; Wang, X.; Luo, H.; Baker, G. A.; Dai, S. *J. Am. Chem. Soc.* **2009**, *131*, 4596−4597.
(24) Yang, W.; Fellinger, T.-P.; Antonietti, M. *J. Am. Chem. Soc.* **2010**, *133*, 206−209.
(25) Li, X.-H.; Wang, X.; Antonietti, M. *Chem. Sci.* **2012**, *3*, 2170−2174.
(26) Wang, Y.; Yao, J.; Li, H.; Su, D.; Antonietti, M. *J. Am. Chem. Soc.* **2011**, *133*, 2362−2365.
(27) Murugavel, R.; Walawalkar, M. G.; Dan, M.; Roesky, H. W.; Rao, C. N. R. *Acc. Chem. Res.* **2004**, *37*, 763−774.
(28) Powell, A. B.; Suzuki, Y.; Ueda, M.; Bielawski, C. W.; Cowley, A. H. *J. Am. Chem. Soc.* **2011**, *133*, 5218−5220.
(29) Choi, J.; Yang, H. Y.; Kim, H. J.; Son, S. U. *Angew. Chem., Int. Ed.* **2010**, *49*, 7718−7722.
(30) Kantchev, E. A. B.; O'Brien, C. J.; Organ, M. G. *Angew. Chem., Int. Ed.* **2007**, *46*, 2768−2813.
(31) Wittmann, S.; Schätz, A.; Grass, R. N.; Stark, W. J.; Reiser, O. *Angew. Chem., Int. Ed.* **2010**, *49*, 1867−1870.
(32) Fortman, G. C.; Nolan, S. P. *Chem. Soc. Rev.* **2011**, *40*, 5151−5169.
(33) Li, F.; Hu, J. J.; Koh, L. L.; Hor, T. S. A. *Dalton Trans.* **2010**, *39*, 5231−5241.
(34) Lee, J. S.; Wang, X.; Luo, H.; Dai, S. *Adv. Mater.* **2010**, *22*, 1004−1007.
(35) Lee, J. S.; Luo, H.; Baker, G. A.; Dai, S. *Chem. Mater.* **2009**, *21*, 4756−4758.
(36) Ziemecki, S. B.; Jones, G. A.; Swartzfager, D. G.; Harlow, R. L.; Faber, J. *J. Am. Chem. Soc.* **1985**, *107*, 4547−4548.
(37) Zlemecki, S. B.; Jones, G. A. *J. Catal.* **1985**, *95*, 621−622.
(38) Krishnankutty, N.; Vannice, M. A. *J. Catal.* **1995**, *155*, 312−326.
(39) Radkevich, V. Z.; Senko, T. L.; Wilson, K.; Grishenko, L. M.; Zaderko, A. N.; Diyuk, V. Y. *Appl. Catal., A* **2008**, *335*, 241−251.
(40) Khabashesku, V. N.; Zimmerman, J. L.; Margrave, J. L. *Chem. Mater.* **2000**, *12*, 3264−3270.
(41) Li, X.; Wang, H.; Robinson, J. T.; Sanchez, H.; Diankov, G.; Dai, H. *J. Am. Chem. Soc.* **2009**, *131*, 15939−15944.
(42) Zhang, L.; Xia, Z. *J. Phys. Chem. C.* **2011**, *115*, 11170−11176.
(43) Sanchez-Lopez, J. C.; Donnet, C.; Lefebvre, F.; Fernandez-Ramos, C.; Fernandez, A. *J. Appl. Phys.* **2001**, *90*, 675−681.
(44) Marton, D.; Boyd, K. J.; Al-Bayati, A. H.; Todorov, S. S.; Rabalais, J. W. *Phys. Rev. Lett.* **1994**, *73*, 118−121.
(45) Teschner, D.; Revay, Z.; Borsodi, J.; Havecker, M.; Knop-Gericke, A.; Schlogl, R.; Milroy, D.; Jackson, S. D.; Torres, D.; Sautet, P. *Angew. Chem., Int. Ed.* **2008**, *47*, 9274−9278.
(46) Teschner, D.; Borsodi, J.; Wootsch, A.; Revay, Z.; Havecker, M.; Knop-Gericke, A.; Jackson, S. D.; Schlogl, R. *Science* **2008**, *320*, 86−89.
(47) Crespo-Quesada, M.; Dykeman, R. R.; Laurenczy, G.; Dyson, P. J.; Kiwi-Minsker, L. *J. Catal.* **2011**, *279*, 66−74.
(48) Staben, S. T.; Blaquiere, N. *Angew. Chem., Int. Ed.* **2010**, *49*, 325−328.
(49) Dong, G.; Teo, P.; Wickens, Z. K.; Grubbs, R. H. *Science* **2011**, *333*, 1609−1612.
(50) D'Souza, D. M.; Müller, T. J. J. *Chem. Soc. Rev.* **2007**, *36*, 1095−1108.
(51) Bellarosa, L.; Diez, J.; Gimeno, J.; Lledos, A.; Suarez, F. J.; Ujaque, G.; Vicent, C. *Chem.—Eur. J.* **2012**, *18*, 7749−7765.
(52) Kuwata, S.; Ikariya, T. *Chem.—Eur. J.* **2011**, *17*, 3542−3556.
(53) Liu, X. M.; McAllister, J. A.; de Miranda, M. P.; McInnes, E. J. L.; Kilner, C. A.; Halcrow, M. A. *Chem.—Eur. J.* **2004**, *10*, 1827−1837.
(54) Trofimen., S. *Chem. Rev.* **1972**, *72*, 497−509.
(55) Mohamed Ahmed, M. S.; Kobayashi, K.; Mori, A. *Org. Lett.* **2005**, *7*, 4487−4489.
(56) Stonehouse, J. P.; Chekmarev, D. S.; Ivanova, N. V.; Lang, S.; Pairaudeau, G.; Smith, N.; Stocks, M. J.; Sviridov, S. I.; Utkina, L. M. *Synlett* **2008**, *100*, 100−104.
(57) Liu, J.; Zhang, R.; Wang, S.; Sun, W.; Xia, C. *Org. Lett.* **2009**, *11*, 1321−1324.
(58) Xue, L.; Shi, L.; Han, Y.; Xia, C.; Huynh, H. V.; Li, F. *Dalton Trans.* **2011**, *40*, 7632−7638.
(59) Lang, R.; Wu, J.; Shi, L.; Xia, C.; Li, F. *Chem. Commun.* **2011**, *47*, 12553−12555.
(60) Lang, R.; Shi, L.; Li, D.; Xia, C.; Li, F. *Org. Lett.* **2012**, *14*, 4130−4133.
(61) Xing, Q.; Shi, L.; Lang, R.; Xia, C.; Li, F. *Chem. Commun.* **2012**, *48*, 11023−11025.
(62) Mohamed Ahmed, M. S.; Mori, A. *Org. Lett.* **2003**, *5*, 3057−3060.
(63) Wasilke, J.-C.; Obrey, S. J.; Baker, R. T.; Bazan, G. C. *Chem. Rev.* **2005**, *105*, 1001−1020.
(64) Tietze, L. F. *Chem. Rev.* **1996**, *96*, 115−136.
(65) Negishi, E.-i.; Copéret, C.; Ma, S.; Liou, S.-Y.; Liu, F. *Chem. Rev.* **1996**, *96*, 365−394.
(66) Grotjahn, D. B.; Van, S.; Combs, D.; Lev, D. A.; Schneider, C.; Rideout, M.; Meyer, C.; Hernandez, G.; Mejorado, L. *J. Org. Chem.* **2002**, *67*, 9200−9209.